Journal of Crystal Growth 76 (1986) 263–271
North-Holland, Amsterdam

THERMODYNAMIC CONSIDERATIONS IN THE SYNTHESIS AND CRYSTAL GROWTH OF GaSb

K.B. McAFEE, Jr., D.M. GAY, R.S. HOZACK, R.A. LAUDISE, G. SCHWARTZ and W.A. SUNDER
AT&T Bell Laboratories, Murray Hill, New Jersey 07974, USA

Received 6 February 1986; manuscript received in final form 24 April 1986

We use a newly developed optimization algorithm, the "sticky trust region technique", for Gibbs energy minimization to determine the gaseous species and liquid and solid phases present during the synthesis and crystal growth of GaSb. The growth system involves almost thirty species comprising a gaseous phase and nine condensed species. We model the system as a function of temperature, oxygen and hydrogen pressure in the presence of an SiO_2 crucible. Ga_2O_3 is identified as the most stable contaminant compound and is seen as a phase that floats on the liquid melt during growth. This oxide often prevents the growth of high quality crystals. We show the effects on its thickness of increasing the ambient hydrogen concentration and determine that the SiO_2 crucible is not an important source of the contaminant oxygen except at high temperatures. The Gibbs energy minimization method combined with the newly-developed optimization algorithm is shown to be an efficient tool for evaluating the problems of crystal growth, materials synthesis and purification.

1. Introduction

For the solid state materials scientist, a description of the growth of most crystals typically entails numerous complex chemical equilibria involving many chemical species in both condensed and gas phases. The numerical evaluation of the relative concentrations of the component species under equilibrium growth conditions can be difficult, and as a consequence, crystal growth and the variation of the relevant growth parameters tend to be approached on a somewhat empirical basis. This paper aims to show that a newly developed optimization technique, the "sticky trust region technique", combined with the Gibbs energy minimization method [1,3], makes it easy to deal simultaneously with many chemical species, and that once thermodynamic data are assembled and evaluated, modern computer techniques make it possible to estimate the equilibria important to a crystal growth problem and to model changes in experimental conditions. Indeed, a software package useful for crystal growth thermodynamic calculations of the sort we describe has been developed and is in use on machines ranging from a Cray to an AT&T-6300 PC.

Because of our current interest in the growth of single crystal GaSb as a substrate material for III–V solid solution detectors and for heterostructure lasers at wavelengths further in the IR than InP-based systems [2], we decided to use this system as a test vehicle. Our previous favorable experience in modeling the equilibria involved in the oxidation of $SiCl_4$, $GeCl_4$, etc. in the modified chemical vapor deposition process used to prepare optical fibers suggested that these techniques could usefully be applied to crystal growth problems [1]. Our calculations are sufficiently flexible to address such questions as the role of the silicon dioxide crucible as a potential source of contamination and the stability of various native oxide phases that result from ultra-low oxygen or water concentrations in the growth ambient atmosphere. A comparison of our equilibrium calculations and some experimental observations about the formation and persistence of oxide film "scum" on the liquid GaSb surface will be discussed.

2. Synthesis and growth – experimental procedure and observations

GaSb is typically synthesized by melting together Ga and Sb at a temperature slightly above

0022-0248/86/$03.50

the melting point of GaSb (705–710°C) in a vitreous SiO_2 crucible. The generally used physical conditions of synthesis and growth are listed in table 1.

The slight excess of antimony is part of the standard growth "recipe" [2] to compensate for Sb volatilization and help preserve the stoichiometry of the grown crystal. The higher number of H_2 moles (1.114) assumes 10 h of flow at the given conditions. This requires a rapid interdiffusion of gases in the reactor chamber. The lower H estimate assumes only ~ 1% of the H is effective as a reducing agent because of poor mixing and a slow approach to equilibrium. The estimated level of oxygen is given over a wide range because of uncertainties in impurity levels. The sources of oxygen include water in the hydrogen ambient gas, the result of outgassing of surfaces, and oxygen present in the reactants, Ga and Sb. An estimate of 10^{-5} moles of O assumes the main source of O is H_2O contamination in the H_2. If the main source of O is adsorbed O in the system, the quantity is then hard to estimate but is certainly much larger. We have taken 10^{-2} moles as an upper limit. Melts are almost always observed to have a "scum" floating on their surface. Grown crystal boules after one pull have approximately half of their surface covered with a "matte finish" layer with the remainder of the surface relatively shiny. The time at the melting point for the first pull is 5–10 h.

Auger spectroscopy shows that a few tens of ångströms of a surface film of gallium and antimony oxides cover the shiny region of the boule. This thin oxide layer is formed after growth by exposure to the laboratory ambient atmosphere. About twice that thickness occurs in the "matte" region. The "thick" oxide is mainly gallium oxide and forms at the melting conditions in the crystal puller atmosphere. If the boule is sandblasted and etched to remove the oxides and remelted, negligible scum is then observed on the melt and a single crystal is normally pulled. This crystal usually has no matte regions. If the polycrystalline boule is remelted without sandblasting, scum is again present on the liquid melt and a single crystal usually cannot be obtained even on the second pull. The time at the melting point for the "second pull" is 5–10 h. During a typical synthesis or growth, the crucible weight loss is negligible ($\leqslant 0.2$ mg). The H_2 carrier gas is passed through a Pd diffuse to remove O_2 and H_2O, which are then below 1 ppm. From the above, we have estimated in table 1 the number of moles of the various constituent molecules present during synthesis and crystal growth conditions.

Table 1

Atmosphere	H_2: 1.114–0.01 moles of H_2
Pressure	1.68 atm
H_2 flow rate	45.0 cm^3/min
Oxygen (impurity)	10^{-2}–10^{-5} mol
Gallium	1.148 mol
Antimony	1.149 mol
SiO_2 crucible	24.676 g
Pull rate	1.2 cm/h

3. Modelling the system: Gibbs energy minimization method, sticky trust region technique and choice of components and species

To calculate the concentration of species present during crystal growth we have used the method of minimizing the Gibbs energy for the multi-phase system. The general mathematical procedures used before the present work to determine equilibrium chemical concentrations are summarized by Van Zeggeren and Storey [3]. All methods of determining chemical equilibria under constant pressure conditions are ultimately alike in minimizing the Gibbs energy:

$$G = \sum_i g_i n_i, \tag{1}$$

where G is the Gibbs free energy, g_i is the chemical potential of species i, and n_i is the number of moles of each component in the system. The familiar "equilibrium constant method" also minimizes G but it is unsuitable for our purpose. While it is theoretically possible to solve simultaneously the many chemical equations that are required to describe the equilibrium of our system, severe and ultimately controlling technical problems with the equilibrium constant method prevent its application.

The difficulties that constrain the use of the equilibrium constant method arise because solutions are not possible if the concentration of any input species becomes 0. In modeling multicomponent solid–liquid systems it is often not possible, a priori, to know which species will have precisely zero concentration. Of course, gas phase equilibria do not pose a problem since small but finite concentrations of gaseous species are always predicted to occur. The problem arises for solid and liquid species in condensed phases that must be modeled in a crystal growth system, since some concentrations will be zero when a phase disappears. To model the concentration of a particular species by the equilibrium constant method, every equilibrium involving that species must be considered. In the present crystal growth case 27 species are required to model the relatively simple binary system involved. Thus, a system of 27 nonlinear equations in 27 unknowns would need to be solved. If the concentration represented by any unknown in that system goes to zero, then that equilibrium must be dropped and the system redefined. The problem is that if several concentration go to zero one can not easily know in advance which equilibria to leave out.

In addition, when one needs to consider solid or liquid solutions such as we have described for $Si_{1-x}Ge_xO_2$ [1,4] and which are pervasive in III–V semi-conductor preparation, then with the equilibrium constant method, x must be known a priori or one must deal with many successive iterations. Cases of mutual solubility of the individual components in III–V crystal growth are important and a flexible method of handling them in the calculations is essential. As we shall see, this is easy when the Gibbs energy is minimized by the technique that we now describe.

As a superior alternative to the equilibrium constant method, we have employed a new optimization technique that applies to any problem having linear equality or inequality constraints (in our case these are the atomic conservation equations), where the objective function (i.e. the Gibbs free energy) has a well-behaved second derivative. Application of the method to a multicomponent system has been recently described [4]. We call this method the "sticky trust region technique [5], STRT". The newly developed method significantly extends and supersedes our earlier use of the "method of element potentials", which we found effective for systems with up to two phases. Because of the multiple phases and components involved in the crystal growth of III–V semiconductors, many species and equilibria need to be considered simultaneously.

The novelty of the STRT, described in detail in ref. [5], lies in the computation of its trial steps. Briefly, a sequence of iterates is computed, each being a vector of values for all the species, such that the corresponding total Gibbs free energy gets smaller and smaller. To obtain a new iterate (one that reduces the Gibbs energy), it is necessary to consider one or more trial iterates, each based on a second-order Taylor series model of the total Gibbs energy about the current iterate. The iterates are chosen to approximately minimize the Taylor series model on the current trust region, a region about the current iterate within which the algorithm believes the model reliably approximates the Gibbs function. Trial iterates are chosen by a strategy that allows several inequality constraints at once to become inactive and several others to become active. An active constraint is one that holds a concentration at bound during an iteration – we impose a small lower bound on all concentrations to prevent numerical difficulties (see eq. (4) below). The strategy is sticky (compared, say, with the quadratic programming used in some other optimization methods) in that once the trial step computation encounters a bound, it no longer considers allowing that concentration to increase again (during the current step computation). It might appear that degeneracy, i.e., linear dependence of the gradients of the active constraints, could lead the strategy to false convergence, but this pitfall is avoided by a side computation that makes a small step (well within the current trust region) to move some of the species from their lower bounds. The beauty of the method for the experimentalist is that, once the system is formulated and given proper thermodynamic data, one need not be concerned over the sophisticated convergence techniques employed.

As a preliminary step to modeling, one must define the phases, components and species to be

included and for which thermodynamic data must be obtained. In the GaSb system we examined the literature descriptions, took into account our own experimental observations during the synthesis and crystal growth, and made preliminary thermodynamic calculations of phase stability. For III–V semiconductors such as GaSb, we find that for the stoichiometric crystal, two and possibly three condensed phases should be included at temperatures significantly less than the melting point. Thus for the GaSb system we decided Ga(ℓ), Sb(ℓ) and GaSb(s) should be considered in equilibrium with Ga(g), Sb(g), Sb_2(g) and Sb_4(g). In our own synthesis experiments we observe liquid gallium when GaSb is heated below the melting point and the calculations of Zakharov and Mirgalovskaya [6] suggest the formation of a liquid phase comprised of antimoney dissolved up to the solubility limit in gallium at temperatures below the melting point along with solid GaSb, Ga and Sb vapors.

In the present study, we decided to neglect corrections to the Gibbs energy of GaSb resulting from defect structures such as Van der Meulen [7] has reported. This effect is not expected to appreciably change the species or phase concentrations we predict, at least at higher temperatures near the melting point of GaSb where gas phase concentrations are probably large compared to solid defect concentrations. However, modeling the defect structure would be useful in that the concentration of defects controls the carrier concentration in undoped material and thermodynamic models connecting defects to experimental parameters would be helpful to the experimentalist endeavoring to control conductivity. In future work we plan to address this problem. Our present thermodynamic model includes the condensed phases GaSb(s), and a solution of Ga(ℓ) containing Sb(ℓ). Currently, we believe our calculations of vapor pressure to be accurate within a factor of 2. We would need more accurate thermodynamic data to increase this reliability.

Because of the likelihood of crucible reactions during synthesis and growth, we have included the reactions of elements present in the crucible as well as in the carrier gases in our model. Both hydrogen (the ambient gas), silicon and oxygen (from the crucible) and oxygen and H_2O that unavoidably entered the system are included. Therefore, the fundamental atomic species that we use as our basis set are Ga, Sb, H, O, and Si. A total of twenty-seven compounds of these elements that we judged to be important were included in our calculations.

Our calculation can be described in eqs. (2) and (3) below:

$$P = \frac{\sum_{i \text{ in gases}} n_i RT}{V - \sum_{j \text{ in solids and liquids}} \rho_j n_j}, \tag{2}$$

$$G = \sum_{i \text{ in gases}} n_i \left[g_i^0 + RT \left(\ln P + \ln \frac{n_i}{\sum_{j \text{ in gases}} n_j} \right) \right] + \sum_{i \text{ in solids}} n_i \left(g_i^0 + \rho_i P \right) + \sum_{i \text{ in liquids}} n_i \left(g_i^0 + \rho_i P + RT \ln \frac{n_i}{\sum_{j \text{ in liquids}} n_j} \right) + G_m^E, \tag{3}$$

where G is the Gibbs energy of the system, which will be minimized by STRT as described above, G_m^E is the excess Gibbs energy of mixing, discussed below, P is the total pressure, T is the temperature, V is the total volume, n_i is the number of moles of species i; ρ_i is the molar volume of condensed species i, and g_i^0 the Gibbs energy of a species under standard conditions.

Note that the $\ln(n_i/\Sigma_j n_j)$ terms of eq. (3) are the familiar mixing entropy. The liquids in (3) include only Ga(ℓ) and Sb(ℓ), i.e., SiO_2(ℓ) is treated as a solid in (3), since the SiO_2 crucible is a glass and its weight loss is significant. The liquid entropy of mixing thus represents the "mixing" contribution to G from Ga(ℓ) solutions containing Sb(ℓ); $n_{Sb(\ell)}$ is the amount of Sb in the Ga solution.

G_m^E is defined in Panish and Ilegems [8]. In the case at hand, it takes the form

$$G_m^E = \alpha \left(\frac{n_{Ga(\ell)} n_{Sb(\ell)}}{n_{Ga(\ell)} + n_{Sb(\ell)}} \right),$$

where α is a function of temperature: $\alpha = \alpha(T) = A - BT$. We obtained A and B by fitting the solubility data of several authors that are shown in ref. [8]: we found $A = 3619.89$ cal and $B = 5.95174$ cal/K, which is in reasonable agreement with the values derived by Panish and Ilegems ($A = 4700$, $B = 6$) using the entropy of fusion equation. The calculations for figs. 2–5 did not include G_m^E; they were done before we made provision for G_m^E, and we believe G_m^E would have little effect on figs. 2–5, since our calculations show that liquid Ga is not stable in the presence of O.

Brebrik, Kaufman, and coworkers [9] have further studied liquidus composition in III–V compounds. However, we have chosen to use the experimental data collected by Panish and Ilegems [8] because we could directly verify their derived data by comparing it with the measured data points they plotted in ref. [8].

To obtain the concentration of all species under equilibrium conditions, we minimize the function G of eq. (3) subject only to the constraints that

$$n_i \geqslant 10^{-13} \text{ moles} \tag{4}$$

Table 2

Species	Mol.wt.	Enthalpy of formation (kcal/mol)	$S°$ (cal/mol·K)	$H - H°$ (kcal/mol)	Gibbs energy [a] at 1000 K (kcal/mol)	References
Gases						
Ar	39.948	0	42.995	3.487	−0.395E+02	[11]
Ga	69.720	66.332	47.871	4.296	0.228E+02	[12]
Ga_2O	155.439	−22.766	82.186	8.238	−0.967E+02	[13]
GaO	85.720	66.802	64.504	5.376	0.767E+01	[12]
GaOH	86.727	−27.390	75.964	9.321	−0.940E+02	[13]
H	1.008	52.103	33.404	3.487	0.222E+02	[11]
H_2	2.016	0	39.700	4.943	−0.348E+02	[11]
H_2O	18.015	−57.795	55.600	6.214	−0.107E+03	[11]
O	15.999	59.554	44.618	3.552	0.185E+02	[11]
O_2	31.999	0	58.190	5.426	−0.528E+02	[11]
OH	17.007	9.318	52.492	5.004	−0.382E+02	[11]
Sb	121.750	63.230	49.070	3.487	0.176E+02	[16]
Sb_2	243.500	55.260	71.600	6.220	−0.101E+02	[16]
Sb_4	487.000	49.360	107.436	13.824	−0.443E+02	[16]
SbH_3	124.774	43.681	67.509	6.886	−0.169E+02	[12]
Si	28.086	107.700	46.296	3.562	0.650E+02	[15]
Si_2	56.172	141.000	66.178	6.713	0.815E+02	[15]
Si_3	84.258	152.000	81.134	10.035	0.809E+02	[15]
SiH_4	32.118	8.200	67.062	11.254	−0.476E+02	[15]
SiO	44.085	−24.300	60.038	5.610	−0.787E+02	[15]
SiO_2	60.085	−72.700	69.698	8.940	−0.133E+03	[15]
Condensed species						
Ga(ℓ)	69.720	0	21.955	5.831	−0.161E+02	[16]
Ga_2O_3(s)	187.438	−260.301	46.935	15.441	−0.292E+03	[12]
GaSb(ℓ)	191.470	−9.990	49.320	24.718	−0.346E+02	[17]
Sb(ℓ)	121.750	2.087	32.386	5.264	−0.250E+02	[16]
Sb(s)	121.750	0.	24.060	9.454	−0.146E+02	[12,16]
Sb_2O_4(s)	307.498	−216.898	63.548	19.224	−0.261E+03	[12]
Sb_2O_5(s)	323.495	−232.290	112.820	48.091	−0.297E+03	[12,14]
Sb_4O_6(s)	582.996	−338.695	117.441	34.012	−0.422E+03	[12]
SiO_2(ℓ) [b]	60.084	−215.740	28.550	10.341	−0.234E+03	[15]

[a] Excluding log(P) terms.

[b] Data used for amorphous SiO_2 crucible.

for all species i and that the number of atoms of each element be constant.

4. Thermodynamic data

Table 2 lists the species used in our calculation as well as our sources for the thermodynamic data. All the data can be considered to be of high quality, except perhaps the data from refs. [13] and [14], which we have been unable to verify. The data listed for $Ga_2O_3(s)$ are of special importance since of all the oxides included in our study we find that compound to be favored. Argon is included in our calculations to allow an easy determination of the change in volume of the system during the calculation. It plays no chemical role. Ionized species are ignored since they are found to be unimportant at the temperatures of crystal growth (~ 1200 K).

The literature has other sources for the data in table 2. We based our selection of sources on comparative evaluation, verifiability, discussions with colleagues, and our own judgements.

5. Results

5.1. Vapor pressure of GaSb

We have considered the equilibrium that is obtained from the compounds listed in (5):

$$\mathrm{GaSb(s)},\ \mathrm{Ga}(\ell),\ \mathrm{Sb}(\ell),\ \mathrm{Ga(g)},\ \mathrm{Sb(g)},\ \mathrm{Sb_2(g)},\ \mathrm{Sb_4(g)}. \quad (5)$$

Fig. 1 shows the vapor pressures of the volatile species over GaSb. Our Ga and Sb_4 pressures agree only approximately with ref. [6] up to about 1000 K. Zakharov and Mirgalovskaya [6], however, neglected Sb_2, which is the major species (except between 1000 and 1100 K), and Sb, which has significant pressure; thus we think our pressure data are more reliable. Chao and Mo [10] also measured what appears to be the total pressure of Sb at three temperatures between 950 and 1050 K; their points fall almost exactly on our Sb_4 pressure curve. We could find no other experimental vapor pressure data.

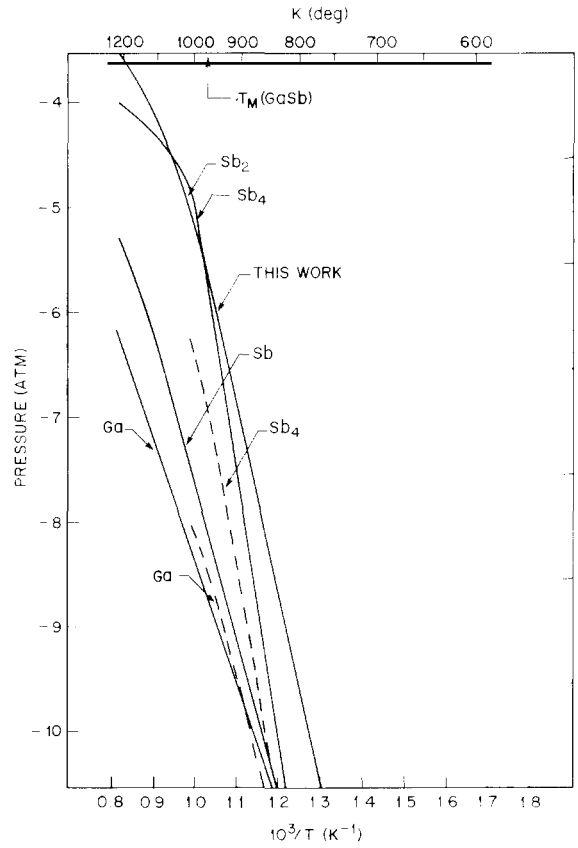

Fig. 1. The vapor pressure of Sb, Sb_2, Sb_4 and Ga above GaSb(s, ℓ) calculated for an equimolar mixture of Ga and Sb. The dashed lines are calculations of Zakharov and Mirgalovskaya [6].

At the melting point the total Sb pressure is about 3.6×10^{-6} Torr and Ga is less than 10^{-9} Torr. This suggests that Sb vacancies are much more likely in the solid than Ga vacancies. The vapor pressure of GaSb may be affected, as discussed in section 3, by the detailed effects of defect structures (non-stoichiometry) and surface energetics.

5.2. Effects of oxygen on the concentration of Ga_2O_3

Fig. 2 shows how oxygen impurity affects the products associated with crystal growth. The Ga/Sb ratio is that used in all our synthesis and growth experiments. H is set at the highest level

likely to represent actual growth conditions. The O level is the midrange of our estimate of that impurity. $Ga_2O_3(s)$ is the significant solid product and persists to temperatures close to the melting point of GaSb, while oxides of antimony are not thermodynamically stable under any of the conditions of growth listed in table 1. Our modeling shows that the oxygen level must be increased several orders of magnitude before the concentrations of antimony oxides are at all significant. The calculations show that the presence of oxygen at the level of 0.001 moles and above can have serious effects on crystal growth. For example, if 0.001 moles of oxygen atoms in all forms are present (6×10^{-4} mole fraction in the entire system), and the temperature is 1000 K, then the amount of Ga_2O_3 produced corresponds to a thickness of the $Ga_2O_3(s)$ surface layer of about 50 Å on the melt. If the oxide so formed is incorporated as an oxide on the entire crystal surface the thickness would be about 10 Å. This is the same order of magnitude as the observed films of oxide formed on the grown crystals. Such films cause polycrystalline growth. The situation is even worse at higher oxygen levels and lower H levels, as we will show below in figs. 4 and 5.

Examination of the fig. 2 shows that a strongly temperature-dependent equilibrium of the gallium oxides and hydrogen occurs and that $Ga_2O_3(s)$ is reduced to $Ga_2O(g)$ and GaOH(g) near the melting point of GaSb. GaO(g) is formed but at too low a concentration to be seen in the present figure. It is important to realize that in the presence of hydrogen and oxygen the total pressure of Sb is higher at the melting point than in the clean system shown in fig. 1. In addition, the melt will be slightly poor in Sb(s) because species such as $Sb_4(g)$ and $Sb_2(g)$ are present in larger amounts than $Ga_2O_3(s)$ and $Ga_2O(g)$. No oxides of antimoney are predicted.

5.3. *Effects of oxygen from the silica crucible during GaSb crystal growth*

Both silicon and oxygen are present, of course, in significant amounts in the crucible. Thermodynamics offers a direct way to assess how both atoms affect crystal growth. The method we have used is to repeat the calculation of fig. 2 (oxygen atom impurity level 0.001 moles) with the addition of 10^{-3} moles of silicon dioxide. Ga, Sb and H are at the levels of fig. 2. The amount of O is 3×10^{-3} moles, which is 0.001 moles more than the O introduced by SiO_2. The amount of SiO_2 is set at a level to make SiO_2 a stable oxide phase, as is observed. Indeed the amount chosen is probably more than actually involved since the crucible weight loss is about 10^{-6} moles of SiO_2. With these assumptions, it is possible to see the effects

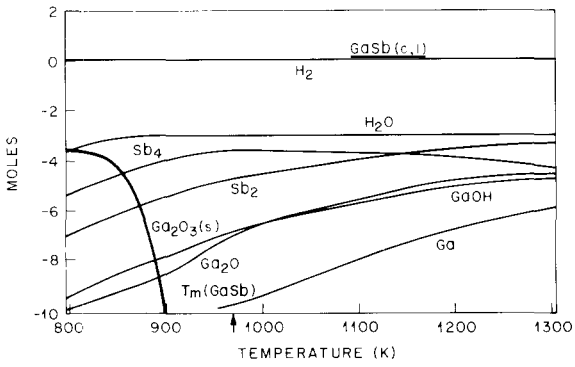

Fig. 2. The molar concentration of various species vs temperature plotted for Ga, Sb, H, O equal to 1.148, 1.149, 2.228 and 0.001 moles, respectively. The pressure is 1.68 atm and the molar concentration of silicon is zero. All species except Ga_2O_3 are gases.

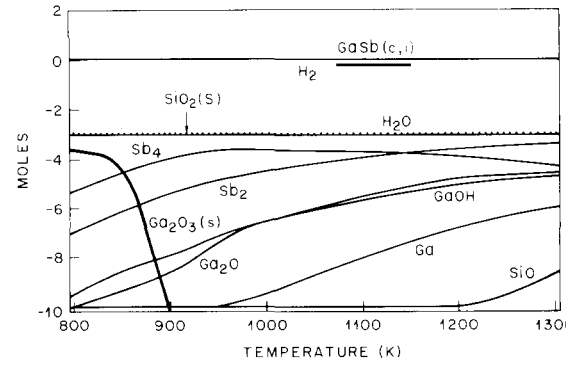

Fig. 3. The molar concentration of the same species plotted with Ga, Sb, H, O, and Si equal to 1.148, 1.149, 2.228, 0.003, 0.001 respectively. Observe that the presence of SiO_2 does not alter the production of $Ga_2O_3(s)$ as compared with fig. 2. All species except Ga_2O_3 are gases.

of the introduction of SiO_2 into the system, as shown in fig. 3. Careful examination of the figure shows that, except at high temperatures where SiO forms, the effect of SiO_2 is negligible. SiO_2 does not decompose and produce significant O at any conditions of importance to crystal growth of GaSb. This is not surprising since the element potential of oxygen (determined from the Gibbs energy of table 1) is much more negative when it combines with Si than with Ga. Around 1200 K the increasing presence of SiO implies a reaction with the crucible has occurred and consequently the concentrations of various species are changed. The value of the thermodynamic calculation is that it gives a quantitative limit (1200 K) to the temperature that can be safely used without risking significant reaction of container components. Similar calculations can predict the safe silica crucible temperatures for other semiconductor materials. We should point out, however, that since accurate thermodynamic data to describe the incorporation of Si and O in GaSb(s) are lacking, we cannot model their incorporation, which may be of great importance in determining the electrical properties of GaSb.

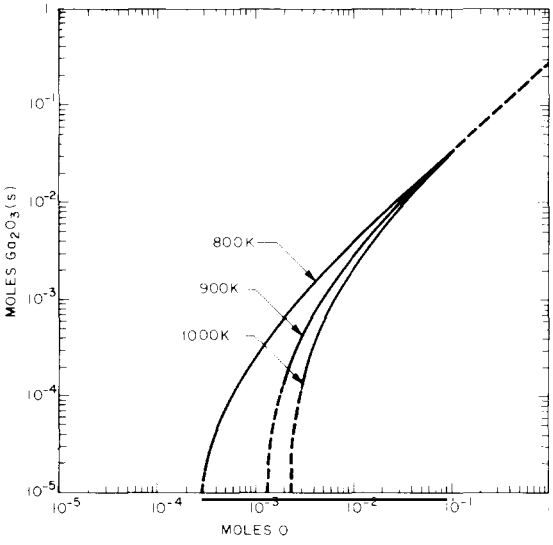

Fig. 4. The molar concentration of Ga_2O_3(s) as a function of oxygen level and temperature. The levels of elements other then oxygen are identical to those of fig. 2.

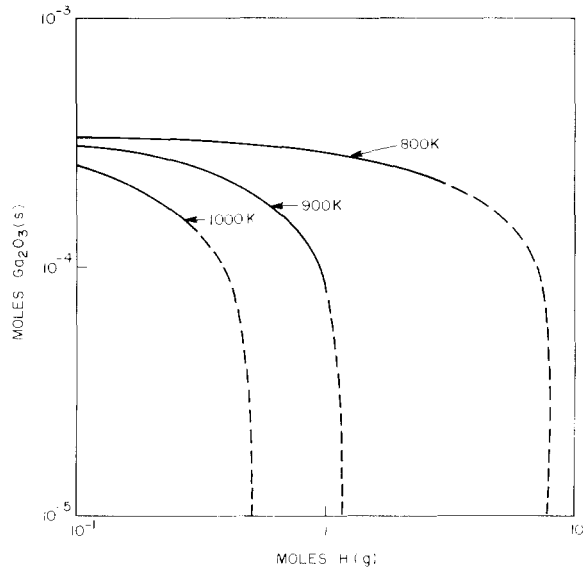

Fig. 5. The reduction of Ga_2O_3(s) as a function of temperature and ambient hydrogen is shown. The concentrations of species other then hydrogen are equal to those of fig. 2.

5.4. Ga_2O_3 dependences on oxygen impurity level

The quantitative formation of Ga_2O_3(s) from impurity oxygen is shown in fig. 4 as a function of temperature near the melting point. For our experimental conditions it should be noted that 10^{-3} moles of atomic oxygen correspond to a film of Ga_2O_3(s) roughly 50 Å thick on the melt at 1000 K. This thickness is calculated for the case where the ambient hydrogen is 2.228 moles. Fig. 4 shows that oxygen impurity can produce unfavorable growth conditions. We experimentally observe a Ga_2O_3 layer of about 50 Å; this suggests that the O level is about 10^{-3} moles. At the melting point an oxygen level of 10^{-2} moles would produce about 10 times more Ga_2O_3 while an oxygen level of 10^{-4} moles would produce about 10 times less Ga_2O_3.

5.5. Effect of hydrogen ambient on Ga_2O_3 formation

Fig. 5 shows how hydrogen affects the formation of Ga_2O_3. At 2.228 moles of H (our upper limit estimate) Ga_2O_3 is well below 10^{-7} moles, i.e., not observable. At the melting point with H at 0.02 moles, about 3×10^{-4} moles of Ga_2O_3 are

produced. Thus if only a small fraction of the H_2 passing through the crystal puller is effective in reducing $Ga_2O_3(s)$, we would expect to find an oxide layer on the melt and grown crystals.

In a recent experiment we have held a GaSb melt in a flowing H_2 atmosphere at 1150 K for 24 h. The area of matte surface of the boule was greatly reduced, thereby showing the H_2 reduction of Ga_2O_3. However, the kinetics of the reduction process must be slow since we were unable to achieve complete elimination of the Ga_2O_3.

6. Discussion and conclusions

This paper is primarily intended to show that modern computer-based thermodynamic calculations combined with an extensive data base can enhance the experimentalist's ability to understand and deal with the complex problems encountered in the growth of crystals.

We have shown that at the melting point of GaSb the principal gas phase species are Sb_4 and Sb_2 when O and H are included, and that water and gallium oxides are the principal additional species. Oxides of Sb are never found under practical experimental conditions. The model predicts that increased H will reduce the oxide films observed in growth, and this result is in qualitative agreement with experiment. We have shown that the films residing on GaSb melt surfaces are primarily oxides in equilibrium and their concentration can be reduced by using hydrogen gas.

We have determined how oxygen from the silica crucible affects the formation of the oxide film. Oxygen remains bound to the silicon and does not form gallium or antimony oxides. Only above 1200 K does SiO_2 decompose to SiO to produce O for reaction with the constituents.

Energy minimization by a robust minimization algorithm, the sticky trust region technique, has been shown to adequately model the composition of the GaSb crystal growth system. We believe it can be applied with confidence to similar problems and extended to MOCVD, defect structure calculations, and gettering.

Acknowledgement

We thank D. Edelson for computational consultation and assistance.

References

[1] K.B. McAfee, Jr., R.S. Hozack, and R.A. Laudise, J. Lightwave Technol. LT-1 (1983) 555.
[2] W.A. Sunder, R.L. Barns, T.Y. Kometani, J. Parsey and R.A. Laudise, J. Crystal Growth, submitted.
[3] F. Van Zeggeren and S.H. Storey, The Computation of Chemical Equilibrium (Cambridge University Press, 1970).
[4] K.B. McAfee, Jr., D.M. Gay, L. Walker and R.S. Hozack, J. Am. Ceram. Soc. 72 (1985) 359.
[5] D.M. Gay, A Trust Region Approach to Linearly Constrained Optimization, in: Numerical Analysis, Proc., Dundee, 1983, Lecture Notes in Mathematics, Ed. D.F. Griffiths (Springer, Berlin, 1984).
[6] Yu. T. Zakharov and M.S. Mirgalovskaya, Inorg. Mater. 3 (1967) 1739.
[7] Y.T. Van der Meulen, J. Phys. Chem. Solids 28 (1967) 25.
[8] M.B. Panish and M. Ilegems, Phase Equilibria in Ternary III–V Systems, in: Progress in Solid State Chemistry, Vol. 7, Eds. H. Reiss and J.O. McCaldin (Pergamon, Oxford, 1972) pp. 39–83.
[9] P.K. Liao, Ching-Hua Su, R.F. Brebrik and L. Kaufman, CALPHAD 7 (1983) 207.
[10] Chao Peng Nien and Mo Chin Chi, Acta Met. Sinica 8 (1965) 32;
see also P. Nougaret and A. Potier, J. Chim. Physique, Physico-Chim. Biol. 66 (1969) 764.
[11] D.R. Stull et al., JANAF Thermochemical Tables, 2nd ed. [NSRDS-NBS37, Natl. Bur. Std. Ref. Data System, Natl. Bur. Std. US 37 (1971)].
[12] D.D. Wagman et al., The NBS Tables of Chemical Thermodynamic Properties [J. Phys. Chem. Ref. Data 11, Suppl. 2 (1982)].
[13] L.V. Gurvich et al., Thermodin. Svoistva Individual'nykh Veshchestv, Vol. III (Akad. Nauk SSSR, 1981).
[14] O. Kubaschewski and C.B. Alcock, Metallurgical Thermochemistry, 5th ed. (Pergamon, Oxford, 1979).
[15] JANAF Thermochemical Tables, Magnetic Tape Version, Suppl. 55. Midland, MI: M.W. Chase, Dow Chemical Co. (1982).
[16] R. Hultgren et al., Selected Values of the Thermodynamic Properties of the Elements (American Society for Metals, Cleveland, OH, 1973).
[17] R. Hultgren et al., Selected Values of the Thermodynamic Properties of Binary Alloys (American Society for Metals, Cleveland, OH, 1973).